

# Tidal wave in $^{102}\text{Pd}$ : An extended five-dimensional collective Hamiltonian description

Y. Y. Wang,<sup>1</sup> Z. Shi,<sup>1</sup> Q. B. Chen,<sup>2</sup> S. Q. Zhang,<sup>2,\*</sup> and C. Y. Song<sup>1,†</sup>

<sup>1</sup>*School of Physics and Nuclear Energy Engineering and International Research Center for Nuclei and Particles in the Cosmos, Beihang University, Beijing 100191, China*

<sup>2</sup>*State Key Laboratory of Nuclear Physics and Technology, School of Physics, Peking University, Beijing 100871, China*

(Dated: April 15, 2016)

The five-dimensional collective Hamiltonian based on the covariant density functional theory is applied to investigate the observed tidal wave mode in the yrast band of  $^{102}\text{Pd}$ . The energy spectra, the relations between the spin and the rotational frequency, and the ratios of  $B(E2)/J(I)$  in the yrast band are well reproduced by introducing the empirical  $ab$  formula for the moments of inertia. This  $ab$  formula is related to the fourth order effect of collective momentum in the collective Hamiltonian. It is also shown that the shape evolution in the tidal wave is determined microscopically by the competition between the rotational kinetic energy and the collective potential in the framework of the collective Hamiltonian.

PACS numbers: 21.10.Re, 21.60.Ev, 27.60.+j, 21.60.Jz

## I. INTRODUCTION

Over the past two decades, novel nuclear excitation modes, such as the magnetic [1–5] and antimagnetic [3, 6] rotations in near spherical nuclei, and the wobbling [7, 8] and chiral [3, 9–11] motions in the triaxially deformed nuclei, have attracted significant attention and extensively been explored from both the experimental and theoretical sides. Recently, another novel nuclear excitation mode, named as the “tidal wave,” has gradually come into people’s vision and attracts new attention [12–16].

As illustrated in Ref. [14], for a quadrupole vibrating droplet of an ideal liquid, there are a family of flow patterns with the same energy, differing by their angular momenta. In the family, there are two limits. One limit is the oscillating motion with no angular momentum carrying and the other is the traveling wave with maximal angular momentum ( $2n\hbar$ , where  $n$  denotes the phonon number) carrying. For a latter case, the surface rotates with a constant angular velocity as in the case of the rotation of a rigid body. This is the so-called tidal wave mode [14]. For a finite nuclear system, this mode is expected to appear in a vibrational or transitional nucleus and corresponds to its yrast mode.

The concept of the tidal wave is of particular concern since it provides a new mechanism for the generation of the angular momentum. Compared with a rigid rotor, where the energy and the angular momentum increase with the rotational angular frequency, the energy and the angular momentum in a tidal wave mode increase with the amplitude of the surface vibration but its frequency remains nearly constant. Quantally the increase of the amplitude of the tidal wave corresponds to the condensation of the phonons [14]. For a quadrupole tidal wave,

it is due to the condensation of quadrupole phonons (d-bosons) [14], and for an octupole tidal wave, it is due to octupole phonons (f-bosons) [17].

Experimentally, the tidal wave was first reported in  $^{182}\text{Os}$  [12] and then in  $^{181,183}\text{Os}$  [13], where the spin difference  $\Delta I = 1$  multiphonon vibration sequences based on high spin intrinsic states were interpreted as tidal waves running over a triaxial surface. Subsequently, the alternating parity sequences in  $^{220}\text{Th}$  [18] and  $^{219}\text{Th}$  [19] were regarded as the reflection-asymmetric tidal wave traveling over a spherical core. Very recently, based on the lifetime measurements, the yrast states of  $^{102}\text{Pd}$  were identified to be the tidal wave running over a quadrupole surface [15]. In this nucleus, the energies of the yrast band are nearly equidistant up to spin  $I = 14$ , and the extracted experimental reduced transition probabilities  $B(E2)$  display a monotonic increase with spin, which provides the first clear evidence of the seven boson condensation.

Theoretically, the tidal wave mode was first investigated in the framework of the shell correction version of the tilted axis cranking model (SCTAC) [14]. Using this model, the observed tidal waves in  $^{181,182,183}\text{Os}$  [12, 13] and  $^{102}\text{Pd}$  [15] were well reproduced. Later on, a phenomenological phonon model that includes anharmonic terms was introduced to analyze the rotational and electromagnetic properties of the tidal wave in  $^{102}\text{Pd}$  [20]. It is worth noting that the angular momentum in the cranking model is not a good quantum number, and the electromagnetic transition probabilities could only be treated in a semiclassical manner. Therefore, it is necessary to search for a theoretical model, in which the angular momentum and the electromagnetic transition probabilities are treated in a quantal manner to investigate the tidal waves.

Since its introduction, the covariant density functional theory (CDFT) has achieved great success in exploring the ground state properties of both spherical and deformed nuclei over almost the whole nuclide chart [21–

\*Electronic address: sqzhang@pku.edu.cn

†Electronic address: cysong@buaa.edu.cn

26] on the basis of relativistic energy density functionals without any additional parameters. Normally in these studies of ground-states the static nuclear mean field approximation is adopted. To calculate the excitation energies and electromagnetic transition probabilities of nuclear low-lying spectra, one needs to include the correlations beyond the static mean field through the restoration of broken symmetries and configuration mixing of symmetry-breaking product states. An effective approach is to construct a collective Hamiltonian with collective parameters determined from microscopic self-consistent mean-field calculations. Particularly to include the rotational symmetry restoration and take into account triaxial shape fluctuations, the five-dimensional collective Hamiltonian based on the covariant density functional theory (5DCH-CDFT) has been developed [27, 28]. In this model, five quadrupole dynamical degrees of freedom including the deformation parameters  $\beta$  and  $\gamma$  and the orientation angles  $\Omega = (\phi, \theta, \psi)$  of the nucleus are considered. The broken rotational symmetry in the static mean field is restored by taking all of the possible orientations into account. Meanwhile, the shape fluctuations around the mean-field minima are allowed by constructing the total Hamiltonian on the quadrupole deformation space. The 5DCH-CDFT has been extensively applied to describe the nuclear collective properties, such as the phase transitions [29–33], the shape evolutions [34–38] as well as the low-lying spectra along with the isotopic and isotonic chains in different mass regions [27, 39–43]. For a review, see, e.g., Ref. [28].

Therefore it is interesting to investigate the tidal waves in the vibrational or transitional nuclei by applying the 5DCH-CDFT. On the one hand, it can answer the question whether the 5DCH could well describe this novel excitation mode or not; on the other hand, it might shed light on the tidal wave study from the point of view of the collective Hamiltonian. In this paper, taking  $^{102}\text{Pd}$  as an example, the 5DCH-CDFT is applied to investigate the energy spectra and electromagnetic properties of the tidal wave mode.

The present paper is organized as follows. In Sec. II, a brief introduction to the frameworks of the CDFT and the 5DCH is given, together with a comment on the microscopic basis of 5DCH. In Sec. III, the potential energy surface of  $^{102}\text{Pd}$  obtained by the CDFT, the yrast energy spectra, and the reduced transition probabilities obtained from the 5DCH in comparison with the experimental data are presented. It is found that in order to better describe the tidal wave in  $^{102}\text{Pd}$ , it is necessary to introduce a spin dependent moment of inertia into the 5DCH calculations. By giving the average quadrupole deformation parameters and the probability distributions of collective wave functions, the shape evolution for the tidal wave in  $^{102}\text{Pd}$  is also analysed. Finally, a summary is given in Sec. IV.

## II. THEORETICAL FRAMEWORK

In this section, first, a brief introduction to the theoretical framework of the covariant density functional theory is presented. Then the formalism of the five-dimensional collective Hamiltonian is given together with its derivation from the adiabatic self-consistent collective coordinate (ASCC) method. For a simple case with one collective parameter, the derivation is further extended to include the fourth order of the collective momenta  $\mathbf{p}^4$  in the collective Hamiltonian in the last subsection.

### A. Covariant density functional theory

Detailed formalism of the CDFT could be found in many literatures, such as Refs. [5, 21–26, 28]. The starting point of the CDFT is a general effective Lagrangian density where the nucleons are coupled with either a meson exchange interaction [21–23] or zero-range point-coupling interaction [44–46] as follows:

$$\begin{aligned} \mathcal{L} &= \mathcal{L}^{\text{free}} + \mathcal{L}^{\text{4f}} + \mathcal{L}^{\text{hot}} + \mathcal{L}^{\text{der}} + \mathcal{L}^{\text{em}} \\ &= \bar{\psi}(i\gamma_\mu \partial^\mu - m)\psi - \frac{1}{2}\alpha_S(\bar{\psi}\psi)(\bar{\psi}\psi) - \frac{1}{2}\alpha_V(\bar{\psi}\gamma_\mu\psi)(\bar{\psi}\gamma^\mu\psi) \\ &\quad - \frac{1}{2}\alpha_{TS}(\bar{\psi}\vec{\tau}\psi)(\bar{\psi}\vec{\tau}\psi) - \frac{1}{2}\alpha_{TV}(\bar{\psi}\vec{\tau}\gamma_\mu\psi)(\bar{\psi}\vec{\tau}\gamma^\mu\psi) \\ &\quad - \frac{1}{3}\beta_S(\bar{\psi}\psi)^3 - \frac{1}{4}\gamma_S(\bar{\psi}\psi)^4 - \frac{1}{4}\gamma_V[(\bar{\psi}\gamma_\mu\psi)(\bar{\psi}\gamma^\mu\psi)]^2 \\ &\quad - \frac{1}{2}\delta_S\partial_\nu(\bar{\psi}\psi)\partial^\nu(\bar{\psi}\psi) - \frac{1}{2}\delta_V\partial_\nu(\bar{\psi}\gamma_\mu\psi)\partial^\nu(\bar{\psi}\gamma^\mu\psi) \\ &\quad - \frac{1}{2}\delta_{TS}\partial_\nu(\bar{\psi}\vec{\tau}\psi)\partial^\nu(\bar{\psi}\vec{\tau}\psi) - \frac{1}{2}\delta_{TV}\partial_\nu(\bar{\psi}\vec{\tau}\gamma_\mu\psi)\partial^\nu(\bar{\psi}\vec{\tau}\gamma^\mu\psi) \\ &\quad - \frac{1}{4}F^{\mu\nu}F_{\mu\nu} - e\frac{1-\tau_3}{2}\bar{\psi}\gamma^\mu\psi A_\mu. \end{aligned} \quad (1)$$

In Eq. (1),  $m$  is the nucleon mass,  $e$  the charge unit for protons, and  $A_\mu$  and  $F_{\mu\nu}$ , respectively, the four-vector potential and field strength tensor of the electromagnetic field. For the 11 coupling constants  $\alpha_S$ ,  $\alpha_V$ ,  $\alpha_{TS}$ ,  $\alpha_{TV}$ ,  $\beta_S$ ,  $\gamma_S$ ,  $\gamma_V$ ,  $\delta_S$ ,  $\delta_V$ ,  $\delta_{TS}$ , and  $\delta_{TV}$ ,  $\alpha$  refers to the four-fermion terms,  $\beta$  and  $\gamma$ , respectively, the third- and fourth-order terms, and  $\delta$  the derivative couplings. The subscripts  $S$ ,  $V$ , and  $T$  indicate the symmetries of the couplings, i.e.,  $S$  stands for scalar,  $V$  for vector, and  $T$  for isovector.

In this work, the relativistic density functional PC-PK1 [46] and the density-independent  $\delta$ -force are, respectively, adopted in the particle-hole and particle-particle channels, with pairing correlations treated in the Bardeen-Cooper-Schrieffer (BCS) approximation. The energy density functional for a nuclear system can be self-consistently obtained in terms of local single-nucleon densities and currents [46]:

$$E_{\text{DF}} = \int d^3r \mathcal{E}(\mathbf{r})$$

$$\begin{aligned}
&= \int d^3r \sum_k \nu_k^2 \psi_k^\dagger(\mathbf{r}) (-i\boldsymbol{\alpha} \cdot \mathbf{p} + m) \psi_k(\mathbf{r}) \\
&+ \int d^3r \left( \frac{\alpha_S}{2} \rho_S^2 + \frac{\beta_S}{3} \rho_S^3 + \frac{\gamma_S}{4} \rho_S^4 + \frac{\delta_S}{2} \rho_S \Delta \rho_S \right. \\
&+ \frac{\alpha_V}{2} j_\mu j^\mu + \frac{\gamma_V}{4} (j_\mu j^\mu)^2 + \frac{\delta_V}{2} j_\mu \Delta j^\mu \\
&+ \frac{\alpha_{TV}}{2} \vec{j}_{TV}^\mu (\vec{j}_{TV})_\mu + \frac{\delta_{TV}}{2} \vec{j}_{TV}^\mu \Delta (\vec{j}_{TV})_\mu \\
&\left. + \frac{1}{4} F_{\mu\nu} F^{\mu\nu} - F^{0\mu} \partial_0 A_\mu + e A_\mu j_p^\mu \right), \quad (2)
\end{aligned}$$

in which  $\psi$  denotes the Dirac spinor field of a nucleon. The local densities and currents

$$\rho_S(\mathbf{r}) = \sum_k \nu_k^2 \bar{\psi}_k(\mathbf{r}) \psi_k(\mathbf{r}), \quad (3)$$

$$j^\mu(\mathbf{r}) = \sum_k \nu_k^2 \bar{\psi}_k(\mathbf{r}) \gamma^\mu \psi_k(\mathbf{r}), \quad (4)$$

$$\vec{j}_{TV}^\mu(\mathbf{r}) = \sum_k \nu_k^2 \bar{\psi}_k(\mathbf{r}) \vec{\tau} \gamma^\mu \psi_k(\mathbf{r}), \quad (5)$$

are calculated in the no-sea approximation, i.e., the summation in Eqs. (2) to (5) only runs over all occupied states with positive energies, where  $\nu_k^2$  represents the occupation factors of single-nucleon states.

By minimizing the energy density functional Eq. (2) with respect to  $\bar{\psi}_k$ , one obtains the Dirac equation for the single nucleon:

$$[\gamma_\mu (i\partial^\mu - V^\mu) - (m + S)] \psi_k = 0. \quad (6)$$

To describe nuclei with general quadrupole shapes, the Dirac equation (6) is solved by expanding the nucleon spinors in the basis of a three dimensional harmonic oscillator in Cartesian coordinates. The map of the energy surface as a function of the quadrupole deformation is obtained by imposing constraints on the axial and triaxial quadrupole moments. The method of quadratic constraint uses an unrestricted variation of the function

$$\langle \hat{H} \rangle + \sum_{\mu=0,2} C_{2\mu} (\langle \hat{Q}_{2\mu} \rangle - q_{2\mu})^2, \quad (7)$$

where  $\langle \hat{H} \rangle$  is the total energy, and  $\langle \hat{Q}_{2\mu} \rangle$  denote the expectation values of the mass quadrupole operators:

$$\hat{Q}_{20} = 2z^2 - x^2 - y^2 \text{ and } \hat{Q}_{22} = x^2 - y^2. \quad (8)$$

Here  $q_{2\mu}$  are the constrained values of the quadrupole moments, and  $C_{2\mu}$  the corresponding stiffness constants [47].

With the single-nucleon wave functions, energies, and occupation factors, generated from constrained self-consistent CDFT solutions, one can calculate the collective inertia parameters. By using the Inglis-Belyaev (IB) formula [48, 49], the moments of inertia (MOIs) are

$$\mathcal{I}_k^{\text{IB}} = \sum_{ij} \frac{(u_i v_j - v_i u_j)^2}{E_i + E_j} |\langle i | \hat{J}_k | j \rangle|^2, \quad k = 1, 2, 3, \quad (9)$$

in which  $k$  denotes the principal axis of nucleus, and  $E_i$  and  $E_j$  denote the quasiparticle energy of the quasiparticle states  $|i\rangle$  and  $|j\rangle$ . The summations  $i$  and  $j$  run over the proton and neutron quasiparticle states. Similar to the MOIs, the mass parameters associated with the two quadrupole collective coordinates  $q_0 = \langle \hat{Q}_{20} \rangle$  and  $q_2 = \langle \hat{Q}_{22} \rangle$  can be also calculated in the cranking approximation [50]

$$B_{\mu\nu}(q_0, q_2) = \frac{\hbar^2}{2} [\mathcal{M}_{(1)}^{-1} \mathcal{M}_{(3)} \mathcal{M}_{(1)}^{-1}]_{\mu\nu}, \quad (10)$$

with

$$\mathcal{M}_{(n),\mu\nu}(q_0, q_2) = \sum_{ij} \frac{\langle i | \hat{Q}_{2\mu} | j \rangle \langle j | \hat{Q}_{2\nu} | i \rangle}{(E_i + E_j)^n} (u_i v_j + v_i u_j)^2. \quad (11)$$

## B. Five-dimensional collective Hamiltonian

The collective Hamiltonian, in terms of a few numbers of collective coordinates and momenta, is an efficient method for describing various kinds of large amplitude collective motions, e.g., the shape coexistence [28, 51], the fission [47], and the chiral and the wobbling motions [52–54]. As a phenomenological model, it can be derived from some microscopic methods [51], e.g., the adiabatic time dependent Hartree-Fock (ATDHF) method [47, 55–57], the generate coordinate method (GCM) [47, 58–60], and the ASCC method [61–65].

In the following, the procedure for the derivation of the collective Hamiltonian with the ASCC method is briefly presented. The main concept of the ASCC method is to solve the equations of the self-consistent collective coordinate (SCC) method [66, 67] using an expansion with respect to the collective momentum. The starting point of the SCC method is the time dependent Hartree-Fock (TDHF) equation. By assuming that the TDHF determinantal states could be represented in multi-dimensional classical phase space characterized by a set of collective coordinates  $\mathbf{p} = \{p_1, p_2, \dots\}$  and collective momenta  $\mathbf{q} = \{q_1, q_2, \dots\}$ , the collective Hamiltonian is defined as the expectation value of the nuclear many-body Hamiltonian  $\hat{H}$ ,

$$H_{\text{coll}} = \langle \phi(\mathbf{q}, \mathbf{p}) | \hat{H} | \phi(\mathbf{q}, \mathbf{p}) \rangle. \quad (12)$$

With the adiabatic approximation which assumes the collective motion to be slow compared to single-particle motion in the nucleus, the collective Hamiltonian is expanded in powers of the collective momentum  $\mathbf{p}$ , stopping at the second order,

$$H_{\text{coll}} = \frac{1}{2} \sum_{ij} B_{ij}(\mathbf{q}) p_i p_j + V(\mathbf{q}), \quad (13)$$

where  $B_{ij}(\mathbf{q})$  and  $V(\mathbf{q})$  are the so-called mass parameter and collective potential, respectively. In the framework of the ASCC method, these two quantities are self-consistently obtained by solving the ASCC equations including the moving-frame Hartree-Fock-Bogoliubov (HFB) equation and moving-frame Random Phase Approximation (RPA) equations [61–65]. Here, we would not repeat the corresponding formulas again.

When the ASCC method is applied to describe the collective rotation, vibration, and the couplings between them, the well-known Bohr Hamiltonian [7], or referred to as the 5DCH, can be constructed in terms of the five collective intrinsic variables  $\beta$ ,  $\gamma$ , and Euler angles  $\Omega = \{\phi, \theta, \psi\}$ . The 5DCH is written as

$$H_{\text{coll}} = T_{\text{vib}}(\beta, \gamma) + T_{\text{rot}}(\beta, \gamma, \Omega) + V(\beta, \gamma), \quad (14)$$

with the vibrational kinetic energy

$$T_{\text{vib}} = \frac{1}{2}B_{\beta\beta}\dot{\beta}^2 + \beta B_{\beta\gamma}\dot{\beta}\dot{\gamma} + \frac{1}{2}\beta^2 B_{\gamma\gamma}\dot{\gamma}^2, \quad (15)$$

the rotational kinetic energy

$$T_{\text{rot}} = \frac{1}{2} \sum_{k=1}^3 \mathcal{I}_k \omega_k^2, \quad (16)$$

and the collective potential energy  $V$ . The mass parameters  $B_{\beta\beta}$ ,  $B_{\beta\gamma}$ ,  $B_{\gamma\gamma}$ , and the MOIs  $\mathcal{I}_k$  depend on the collective variables  $\beta$  and  $\gamma$ .

The Hamiltonian (14) is quantized according to the Pauli prescription [68] as

$$\hat{H}_{\text{coll}} = \hat{T}_{\text{vib}} + \hat{T}_{\text{rot}} + V, \quad (17)$$

with

$$\begin{aligned} \hat{T}_{\text{vib}} = & -\frac{\hbar^2}{2\sqrt{wr}} \left\{ \frac{1}{\beta^4} \left[ \frac{\partial}{\partial \beta} \sqrt{\frac{r}{w}} \beta^4 B_{\gamma\gamma} \frac{\partial}{\partial \beta} \right. \right. \\ & \left. \left. - \frac{\partial}{\partial \beta} \sqrt{\frac{r}{w}} \beta^3 B_{\beta\gamma} \frac{\partial}{\partial \gamma} \right] + \frac{1}{\beta \sin 3\gamma} \left[ -\frac{\partial}{\partial \gamma} \right. \right. \\ & \left. \left. \times \sqrt{\frac{r}{w}} \sin 3\gamma B_{\beta\gamma} \frac{\partial}{\partial \beta} + \frac{1}{\beta} \frac{\partial}{\partial \gamma} \sqrt{\frac{r}{w}} \sin 3\gamma B_{\beta\beta} \frac{\partial}{\partial \gamma} \right] \right\}, \end{aligned} \quad (18)$$

and

$$\hat{T}_{\text{rot}} = \frac{1}{2} \sum_{k=1}^3 \frac{\hat{J}_k^2}{\mathcal{I}_k}, \quad (19)$$

where  $\hat{J}_k$  denotes the components of the angular momentum in the body-fixed frame of a nucleus. The two quantities that appear in the expression (18) for the vibrational energy are  $r = D_1 D_2 D_3$  and  $w = B_{\beta\beta} B_{\gamma\gamma} - B_{\beta\gamma}^2$ , where the inertial parameters  $D_k$  are related to the MOIs  $\mathcal{I}_k$  as,

$$\mathcal{I}_k = 4D_k \beta^2 \sin^2 \left( \gamma - \frac{2k\pi}{3} \right), \quad k = 1, 2, 3. \quad (20)$$

The corresponding eigenvalue problem is solved using an expansion of eigenfunctions in terms of a complete set of basis functions that depend on the deformation variables  $\beta$  and  $\gamma$  and the Euler angles  $\phi$ ,  $\theta$ , and  $\psi$  [69]. The diagonalization of the Hamiltonian yields the excitation energies and collective wave functions:

$$\Psi_{\alpha}^{IM}(\beta, \gamma, \Omega) = \sum_{K \in \Delta I} \psi_{\alpha K}^I(\beta, \gamma) \Phi_{MK}^I(\Omega). \quad (21)$$

where the summation is over the allowed set of  $K$  values:

$$\Delta I = \begin{cases} 0, 2, \dots, I & \text{for } I \bmod 2 = 0 \\ 2, 4, \dots, I-1 & \text{for } I \bmod 2 = 1. \end{cases} \quad (22)$$

Using the collective wave functions (21), various observables can be calculated and compared with experimental data. For the quadrupole  $E2$  reduced transition probability, it is calculated as

$$B(E2 : \alpha I \rightarrow \alpha' I') = \frac{1}{2I+1} |\langle \alpha' I' || \hat{\mathcal{M}}(E2) || \alpha I \rangle|^2, \quad (23)$$

where  $\hat{\mathcal{M}}(E2)$  denotes the electric quadrupole operator; see Ref. [70] for details.

In the framework of 5DCH-CDFT, all the collective parameters are determined by the CDFT calculations. That is, the collective potential energy  $V$  is given by the constrained CDFT calculations in the  $\beta$ - $\gamma$  plane; meanwhile the moments of inertia  $\mathcal{I}_k$  and the mass parameters  $B_{\beta\beta}$ ,  $B_{\beta\gamma}$ ,  $B_{\gamma\gamma}$  may be approximately given by the cranking formulas (9) and (10), respectively.

### C. A comment on expansions in the collective momentum

As stated in the last subsection, the collective Hamiltonian can be derived from the ASCC method by expanding the collective momenta up to the second order. It should be noticed that, as commented on in Ref. [57], the adiabatic assumption is actually vital to the phenomenological forms of the collective model, since the kinetic energy would not be quadratic otherwise, except in the trivial case of translations. However, there is no reason why the energy in the collective model should turn out to be a quadratic function of the collective momenta or the velocities in general. The only way to get it to be quadratic is by assuming that the velocities are small and by expanding the energy in powers of them, stopping at the second order [57].

Although the collective Hamiltonian with this assumption has achieved lots of successes, it was found that the collective Hamiltonian could not well describe the energy spectra for the weakly deformed transitional nuclei when the spin is large [27]. This fact might suggest that the expansion of the collective Hamiltonian in collective momentum up to the second order is not necessarily enough. It would be therefore interesting to study the contributions of the higher-order terms of the collective momenta.

As an initial try, we take the fourth order of the collective momentum  $p^4$  into account in the collective Hamiltonian. For simplicity, we consider the one dimensional case; then the Eq. (13) becomes

$$H_{\text{coll}} = \frac{1}{2!}B_2(q)p^2 + \frac{1}{4!}B_4(q)p^4 + V(q). \quad (24)$$

Following the procedure of deriving the ASCC equations in Ref. [61], the mass parameters  $B_2(q)$ ,  $B_4(q)$ , and the collective potential  $V(q)$  in Eq. (24) are now calculated by

$$V(q) = \langle \phi(q) | \hat{H} | \phi(q) \rangle, \quad (25)$$

$$B_2(q) = \left. \frac{\partial^2 H_{\text{coll}}}{\partial q^2} \right|_{p=0} = -\langle \phi(q) | \hat{Q}, [\hat{Q}, \hat{H}] | \phi(q) \rangle, \quad (26)$$

$$B_4(q) = \left. \frac{\partial^4 H_{\text{coll}}}{\partial q^4} \right|_{p=0} = \langle \phi(q) | [\hat{Q}, [\hat{Q}, [\hat{Q}, [\hat{Q}, \hat{H}]]]] | \phi(q) \rangle, \quad (27)$$

where  $\hat{Q}$  is the infinitesimal generator defined at the collective state  $|\phi(q)\rangle$

$$\hat{Q}|\phi(q)\rangle = \left. \frac{1}{i} \frac{\partial |\phi(q, p)\rangle}{\partial p} \right|_{p=0}. \quad (28)$$

If we neglect the residual two-body interaction in the Hamiltonian  $\hat{H}$ , the mass parameters are reduced to the cranking formulas,

$$B_2^{-1}(q) = 2 \sum_{mi} \frac{|\langle m | \frac{\partial \hat{H}_M}{\partial q} | i \rangle|^2}{(\varepsilon_m - \varepsilon_i)^3}, \quad (29)$$

$$B_4^{-1}(q) = 8 \sum_{mi} \frac{|\langle m | \frac{\partial \hat{H}_M}{\partial q} | i \rangle|^4}{(\varepsilon_i - \varepsilon_m)^5}, \quad (30)$$

where  $\hat{H}_M$  is the so-called moving frame Hamiltonian [61]

$$\hat{H}_M(q) = \hat{H} - \frac{\partial V(q)}{\partial q} \hat{Q}, \quad (31)$$

and the  $|m\rangle$ ,  $|i\rangle$  and  $\varepsilon_m$ ,  $\varepsilon_i$  are the eigenstates and the corresponding eigenvalues of  $\hat{H}_M$ . The indices  $m$  and  $i$  denote the particle and hole states, respectively. Noting that  $\varepsilon_m > \varepsilon_i$ , thus the  $B_2^{-1}(q)$  is positive, while  $B_4^{-1}(q)$  is negative.

If one rewrites the collective Hamiltonian (24) as

$$\begin{aligned} H_{\text{coll}} &= V(q) + \frac{1}{2!}B_2(q)p^2 + \frac{1}{4!}B_4(q)p^4 \\ &= V(q) + \frac{1}{2}B_2(q) \left[ 1 + \frac{1}{12} \frac{B_4(q)}{B_2(q)} p^2 \right] p^2 \\ &= V(q) + \frac{1}{2}B(q, p)p^2, \end{aligned} \quad (32)$$

it can be seen that the contributions of the fourth order of  $p$  could be absorbed into a momentum dependent effective parameter

$$B(q, p) = B_2(q) \left[ 1 + \frac{1}{12} \frac{B_4(q)}{B_2(q)} p^2 \right]. \quad (33)$$

According to the above analysis,  $B_2(q)$  is positive and  $B_4(q)$  is negative; therefore  $B(q, p)$  should decrease with respect to the increase of  $p$ .

For considering the fourth order contribution into a rotational kinetic energy with the expression,

$$\hat{T}_{\text{rot}} = \frac{\hat{J}^2}{2\mathcal{I}}, \quad (34)$$

one just needs to replace the  $p$  with  $\hat{J}$ , and  $1/\mathcal{I}$  with

$$\frac{1}{\mathcal{I}} = B(I) = B_2 \left[ 1 + \frac{1}{12} \frac{B_4}{B_2} I(I+1) \right]. \quad (35)$$

In the above expression, the  $\hat{J}^2$  has been replaced by  $I(I+1)$  in the mean-field approximation. Considering that  $B_4$  should be generally far smaller than  $B_2$ ,  $B_4/B_2$  is a small quantity, so that it has

$$\frac{1}{\mathcal{I}} = B_2 \left[ 1 + \frac{1}{12} \frac{B_4}{B_2} I(I+1) \right] \approx \frac{1}{a\sqrt{1+bI(I+1)}}, \quad (36)$$

with

$$a = \frac{1}{B_2}, \quad b = -\frac{B_4}{6B_2}. \quad (37)$$

This immediately shows that the moment of inertia has the form of

$$\mathcal{I} = a\sqrt{1+bI(I+1)}. \quad (38)$$

It is just the well-known  $ab$  formula proposed by Wu and Zeng [71, 72]. From this point of view, the  $ab$  formula of MOI can be microscopically accessed by considering the fourth order term of the collective momentum.

### III. RESULTS AND DISCUSSION

In the CDFT calculations, the point-coupling energy density functional PC-PK1 in the particle-hole channel and the density-independent  $\delta$  force in the particle-particle channel are adopted [46]. The solution of the equation of motion for the nucleons is accomplished by an expansion of the Dirac spinors in a set of three-dimensional harmonic oscillator basis functions in Cartesian coordinates with 12 major shells. To provide the collective parameters on the  $(\beta, \gamma)$  plane for the 5DCH, a constrained triaxial CDFT calculation is carried out in the region  $\beta \in [0.0, 0.8]$  and  $\gamma \in [0^\circ, 60^\circ]$  with step sizes  $\Delta\beta = 0.05$  and  $\Delta\gamma = 6^\circ$ .



In Fig. 1, the potential energy surface in the  $\beta$ - $\gamma$  plane for  $^{102}\text{Pd}$  calculated by the constrained triaxial CDFT is shown. It shows that the minimum of the potential energy surface (PES) (labeled as a red dot) locates at  $(\beta = 0.19, \gamma = 0^\circ)$ , which corresponds to a moderate prolate shape. Around the minimum, the PES exhibits a relatively soft character. The energy difference between the ground state  $(\beta = 0.19, \gamma = 0^\circ)$  and the lowest oblate energy position  $(\beta = 0.15, \gamma = 60^\circ)$  is less than 2.2 MeV.

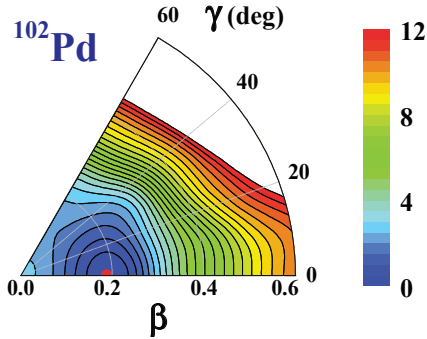


FIG. 1: (Color online) The potential energy surface in the  $\beta$ - $\gamma$  plane ( $0 \leq \gamma \leq 60^\circ$ ) for  $^{102}\text{Pd}$  calculated by the constrained triaxial CDFT with PC-PK1 [46]. All energies are normalized with respect to the binding energy of the absolute minimum (in MeV). The energy between each contour line is 0.5 MeV.

With the collective potential, moments of inertia, and mass parameters determined from the CDFT, the collective energies and collective wave functions can be obtained by diagonalizing the 5DCH at each given spin. It is noted that the MOIs adopted here are obtained by the IB formula (9). It usually underestimates the experimental MOIs due to the absence of the contributions of time-odd fields (the so-called Thouless-Valatin (TV) dynamical rearrangement contributions) [27], the inclusion of which requires much demanding computations. To consider the effect of TV terms, one may multiply a factor  $1 + \alpha$  to the IB MOIs, i.e., the input MOIs for the 5DCH are  $\mathcal{I}_k = \mathcal{I}_k^{\text{IB}}(1 + \alpha)$ ,  $k = 1, 2, 3$  [27, 73]. The value of  $\alpha$  is obtained so that the energy of the  $2_1^+$  state from the 5DCH coincides with the experimental data. The justification of this treatment has been demonstrated for some nuclei in the  $A \sim 190$  mass region [73], while the situation may become considerably complicated especially for nuclei with soft potential energy surfaces [51, 64, 74, 75].

The obtained energy spectra of the yrast band of  $^{102}\text{Pd}$  from the 5DCH (labeled as 5DCH) in comparison with the data [15] are illustrated in Fig. 2. For reference, the harmonic vibrational and rotational limits are also shown in the figure. It is shown that the experimental data are closer to the harmonic than the rotational limit, and the deviation from the harmonic limit indicates the anharmonicity as discussed in Refs. [15, 20]. In the 5DCH calculation, the value of  $\alpha$  is taken as 0.40. As shown in Fig. 2, the 5DCH calculation can reproduce the data for the low spin region ( $I \leq 6\hbar$ ). However, with the increase

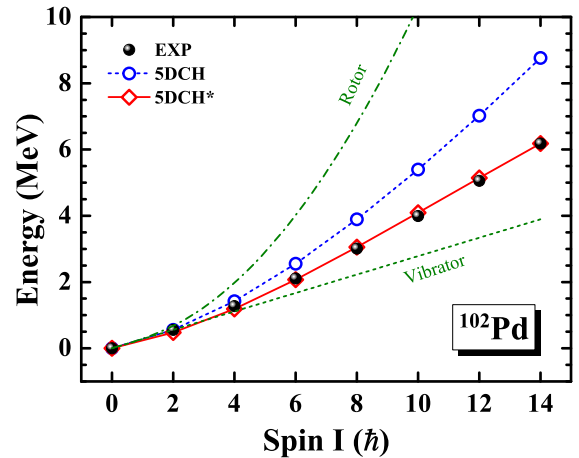


FIG. 2: (Color online) The comparison of the yrast band energy between the experimental data and 5DCH calculations for  $^{102}\text{Pd}$ . The blue circle with the dashed line (5DCH) and the red lozenge with the solid line (5DCH\*) represent the calculations with the MOI corrected by renormalizing the IB effective MOI to the empirical values with a common factor and by the empirical  $ab$  formula, respectively. The harmonic vibrational and rotational limits are shown in dashed and dashed-dotted lines.

of spin, it gradually deviates from the data in value and also from the linear increase of the data. The deviation reaches to 2.5 MeV at  $I = 14\hbar$ , nearly 40% larger than the data. This indicates that the spin-independent MOIs could not describe the energy spectra well for the whole spin region in  $^{102}\text{Pd}$ , whose PES shows a relatively soft character as seen in Fig. 1.

As discussed in Sec. II C, the 5DCH is expanded up to the second order with respect to the collective momentum by using an adiabatic approximation. It is not necessarily enough for the study of the transitional nuclei. It is therefore interesting to investigate the high order effects of collective momenta. As shown in Sec. II C, effectively one can take the fourth order of the collective momentum  $p^4$  into account through a  $p$  dependent inertial parameter ( $\sim p^2$ ). Correspondingly in the present investigation, we introduce a spin dependent MOIs,  $\mathcal{I}_k = a\sqrt{1 + bI(I+1)} = a_0\mathcal{I}_k^{\text{IB}}\sqrt{1 + bI(I+1)}$ , into 5DCH calculations. The parameters  $a_0$  and  $b$  are obtained by fitting the available experimental energy spectra using the least squares method (LSM) with  $a_0 = 1.713$  and  $b = 0.003$ . We will denote this calculation as the 5DCH\*.

The energy spectra of the 5DCH\* are also included in Fig. 2 in comparison with the 5DCH results and the data. It is seen that 5DCH\* results well reproduce the data and the maximal difference is only about 0.1 MeV. In addition, it is demonstrated that the energy spectra show a nearly linear increase with respect to spin. This corresponds to the characteristic energy spectra of a tidal wave [14].

From the energy spectra, the rotational frequency can be extracted according to the classical relations  $\omega =$

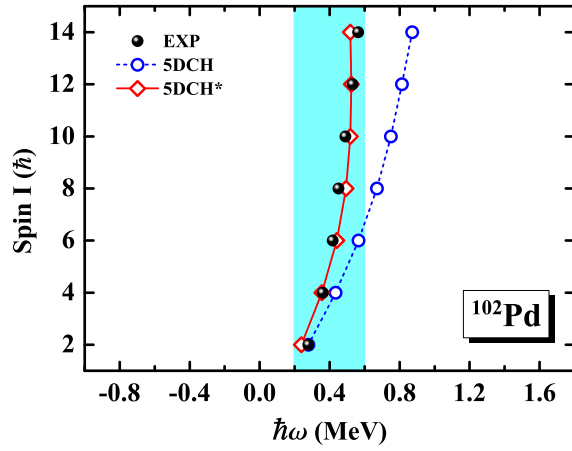


FIG. 3: (Color online) The experimental and theoretical  $I$ - $\hbar\omega$  relation of the yrast band for  $^{102}\text{Pd}$ . The light cyan band represents a region of  $\hbar\omega = 0.2$  to  $0.6$  MeV.

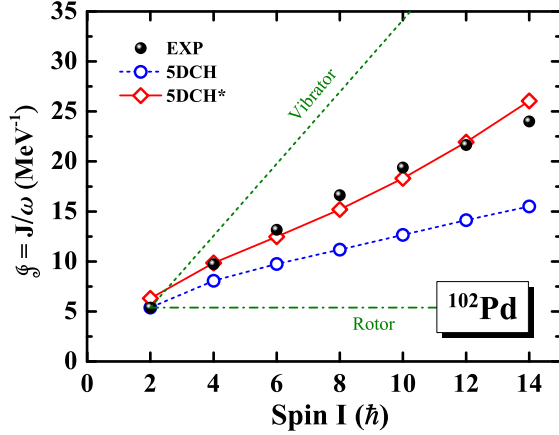


FIG. 4: (Color online) The experimental and theoretical moments of inertia  $\mathcal{J}$  as functions of the spin  $I$  for  $^{102}\text{Pd}$ . The harmonic vibrational and rotational limits are shown in dashed and dashed-dotted lines.

$dE/dI$  as [76]

$$\omega(I) = \frac{\Delta E}{\Delta I} = \frac{1}{2}[E(I) - E(I-2)]. \quad (39)$$

The obtained experimental and theoretical  $I$ - $\hbar\omega$  relations of the yrast band for  $^{102}\text{Pd}$  are shown in Fig. 3. It is seen that the spin increases rapidly with respect to the rotational frequency experimentally. In a very small rotational frequency interval ( $\sim 0.4$  MeV), the spin increases  $12\hbar$ . This implies that the generation of spin is mainly caused by the increase of MOIs rather than the increase of rotational frequency, a significant feature of a tidal wave. The 5DCH\* calculation describes this feature very well. The 5DCH results however show a slow  $I$ - $\hbar\omega$  increase, where  $\hbar\omega$  increases from  $\sim 0.25$  to  $0.85$  MeV with spin from  $2\hbar$  to  $14\hbar$ .

Figure 4 displays the comparison between the experimental and theoretical moments of inertia  $\mathcal{J}$ , obtained

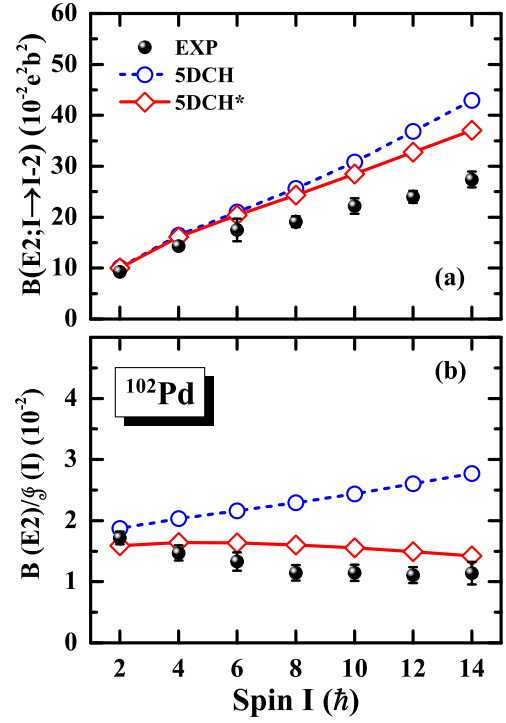


FIG. 5: (Color online) (a): The experimental and theoretical reduced electromagnetic transition probabilities  $B(E2)$  of the yrast band as a function of the spin  $I$  for  $^{102}\text{Pd}$ . (b): The experimental and calculated ratios  $B(E2)/\mathcal{J}$  as a function of the spin  $I$ .

by  $\mathcal{J} = J/\omega$  with

$$\mathcal{J}(I) = \frac{J(I)}{\omega(I)} = \frac{2J(I)}{E(I) - E(I-2)}, \quad J(I) = I - \frac{1}{2}, \quad (40)$$

in which the classical angular momentum  $J$  is associated with the quantal value  $(I-1)+1/2 = I-1/2$  [76]. As seen in Fig. 4, the experimental MOI increases nearly linearly with respect to spin. The 5DCH results give an increasing trend of the MOI but underestimate the increase of experimental values. With the spin dependent MOIs, the 5DCH\* reproduces the data rather well. With the collective wave functions obtained by diagonalizing the 5DCH, the reduced transition probabilities  $B(E2)$  can be calculated according to Eq. (23). The corresponding  $B(E2)$  values from the 5DCH and 5DCH\* are drawn in Fig. 5(a) in comparison with the available data [15]. It is shown that both the 5DCH and 5DCH\* results correctly give the increase trend of the experimental data, but to some extent overestimate the experimental values. Again the 5DCH\* results are closer to the data than those from the 5DCH. It is noted that the monotonic increase of  $B(E2)$  values with spin is another characteristic feature of a tidal wave as demonstrated in Ref. [14], which mainly comes from the increase of the nuclear quadrupole deformation. Considering that in the 5DCH and 5DCH\* calculations the physical observables, such as transition probabilities and spectroscopic quadrupole moments, are calculated

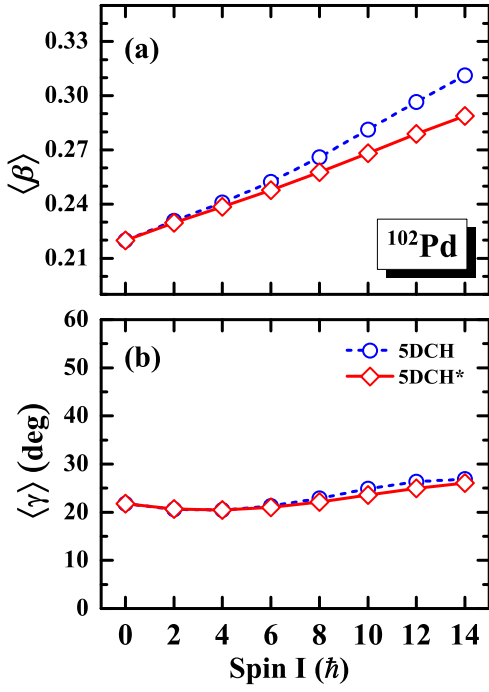


FIG. 6: (Color online): The average values of the quadrupole deformation parameters (a)  $\beta$  and (b)  $\gamma$  calculated by the 5DCH as functions of spin  $I$  for  $^{102}\text{Pd}$ .

in the full configuration space and there are no effective charges, such predictions are appreciable. In Fig. 5(b), the experimental and calculated ratios  $B(E2)/\mathcal{J}$  as functions of spin  $I$  are shown, which are expected to be nearly constant for a tidal wave. This behavior is well shown by the experimental data and also the 5DCH\* results. The 5DCH results, however, give an increase trend of  $B(E2)/\mathcal{J}$  due to the faster increase of the  $B(E2)$  with spin than that of MOI. In fact, the behaviors of  $B(E2)$  and  $B(E2)/\mathcal{J}$  given by the 5DCH and 5DCH\* can be understood by the evolution of obtained deformation parameters with respect to spin, which will be discussed below.

In the 5DCH, the expectation values of the quadrupole deformation  $\langle\beta\rangle$  and  $\langle\gamma\rangle$  for each given state  $|\Psi_\alpha^I\rangle$  are calculated by [27]

$$\langle\beta\rangle_{I\alpha} = \sqrt{\langle\beta^2\rangle_{I\alpha}}, \quad (41)$$

$$\langle\gamma\rangle_{I\alpha} = \frac{1}{3} \arccos \frac{\langle\beta^3 \cos 3\gamma\rangle_{I\alpha}}{\sqrt{\langle\beta^2\rangle_{I\alpha} \langle\beta^4\rangle_{I\alpha}}}, \quad (42)$$

where

$$\begin{aligned} \langle\beta^2\rangle_{I\alpha} &= \langle\Psi_\alpha^I|\beta^2|\Psi_\alpha^I\rangle \\ &= \sum_{K \in \Delta I} \int \beta^2 |\psi_{\alpha,K}^I(\beta, \gamma)|^2 d\tau_0, \end{aligned} \quad (43)$$

$$\begin{aligned} \langle\beta^4\rangle_{I\alpha} &= \langle\Psi_\alpha^I|\beta^4|\Psi_\alpha^I\rangle \\ &= \sum_{K \in \Delta I} \int \beta^4 |\psi_{\alpha,K}^I(\beta, \gamma)|^2 d\tau_0, \end{aligned} \quad (44)$$

$$\begin{aligned} \langle\beta^3 \cos 3\gamma\rangle_{I\alpha} &= \langle\Psi_\alpha^I|\beta^3 \cos 3\gamma|\Psi_\alpha^I\rangle \\ &= \sum_{K \in \Delta I} \int \beta^3 \cos 3\gamma |\psi_{\alpha,K}^I(\beta, \gamma)|^2 d\tau_0. \end{aligned} \quad (45)$$

The calculated  $\langle\beta\rangle$  and  $\langle\gamma\rangle$  as functions of spin  $I$  by the 5DCH and 5DCH\* are shown in Figs. 6(a) and 6(b), respectively. For the  $\beta$  degree of freedom, the average values  $\langle\beta\rangle$  calculated by the 5DCH and 5DCH\* both increase linearly with spin, i.e., from 0.22 at  $I = 0\hbar$  to 0.31 and 0.29 at  $I = 14\hbar$ , respectively, consistent with the increase behavior of  $B(E2)$  shown in Fig. 5(a). For the  $\gamma$  degree of freedom, the average values  $\langle\gamma\rangle$  exhibit slight increases for both the 5DCH and 5DCH\* calculations, i.e., from  $\sim 22^\circ$  at  $I = 0\hbar$  to  $\sim 27^\circ$  and  $\sim 26^\circ$  at  $I = 14\hbar$ , respectively.

It is interesting to note that the shape evolution obtained by the 5DCH is more obvious than that by the 5DCH\*. This can be understood by the formalism of the quantized 5DCH (17), the diagonalization of which naturally leads to the collective states at a given angular momentum and the corresponding distributions in the  $\beta$ - $\gamma$  plane. Since the vibration term  $\hat{T}_{\text{vib}}$  is mainly responsible for the  $\beta$  and  $\gamma$  vibrational excitations, for the yrast band focused here, it can be neglected compared with the other two terms  $\hat{T}_{\text{rot}}$  and  $V$ . Therefore, the shape evolution of the yrast band is mainly determined by the competition between the rotational kinetic energy  $\hat{T}_{\text{rot}}$  and the collective potential  $V$ . In the present 5DCH and 5DCH\* calculations, the collective potential  $V$  does not change with respect to spin, while the rotational kinetic energy  $\hat{T}_{\text{rot}}$  depends on the quadratic of spin  $I(I+1)$  and also the variation of MOIs.

At the beginning of the yrast band, since the angular momentum is small, its equilibrium deformation is mainly determined by the minimum of the collective potential. This explains that the deformation parameters at the region of  $I \leq 4\hbar$  ( $\beta \sim 0.22$ ) are rather close to the deformation parameter of the minimum of the potential energy surface in Fig. 1 ( $\beta \sim 0.20$ ). As the spin increases, the contribution of the kinetic energy becomes gradually important. As it is known, the MOIs increase with respect to  $\beta^2$  [47], i.e., a larger deformation  $\beta$  would make the kinetic energy more energetic favorable. As a result, the increase of spin induces the deformation of the yrast state to be larger. This explains the increase trend of the deformation in the 5DCH as shown in Fig. 6. After introducing the *ab* formula in the 5DCH\*, the input MOIs are enlarged. Accordingly, the driven effect by the kinetic energy to the deformation is reduced. Thus the deformation parameters obtained by 5DCH\* is smaller than the 5DCH ones.

Based on the above analysis, the description of the 5DCH and 5DCH\* for the yrast band of  $^{102}\text{Pd}$  raises a schematic picture of a tidal wave. Here, the performance of the tidal wave mainly depends on the competition between the rotational kinetic energy  $\hat{T}_{\text{rot}}$  and the collective potential  $V$ . For a nucleus with a stiff potential energy surface, its deformation is not easy to change and the



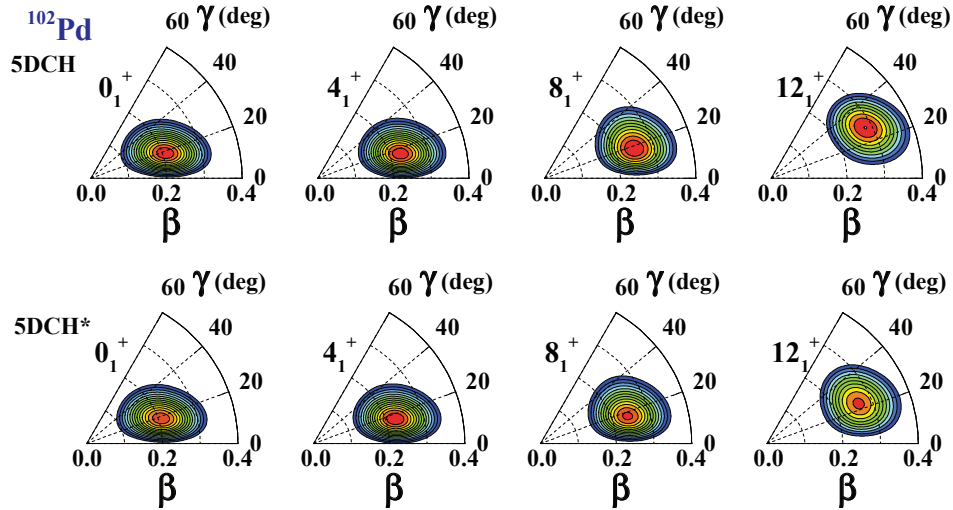


FIG. 7: (Color online) The probability distributions in the  $\beta$ - $\gamma$  plane for the  $0_1^+$ ,  $4_1^+$ ,  $8_1^+$  and  $12_1^+$  states of  $^{102}\text{Pd}$  calculated by the 5DCH and 5DCH\*.

MOIs are nearly spin-independent. Thus the increase of the angular frequency will take charge of the generation of nuclear angular momentum. This corresponds to the rotation of a rigid rotor. For a nucleus with a soft potential energy surface, its deformation is easy to change and the competition between  $\hat{T}_{\text{rot}}$  and  $V$  prefers a larger deformation. Thus the increase of the MOIs contributes to the generation of nuclear angular momentum while the angular frequency may not have an obvious increase. This corresponds to the mode of a tidal wave.

Finally, in Fig. 7, the probability distributions [31] in the  $\beta$ - $\gamma$  plane calculated by the 5DCH and 5DCH\* are displayed for the yrast states  $0_1^+$ ,  $4_1^+$ ,  $8_1^+$  and  $12_1^+$  of  $^{102}\text{Pd}$ . It can be clearly seen that the peaks of probability distributions locate around the deformed points which are consistent with the values of the average deformation parameters shown in Fig. 6. To further compare the difference between the probability distributions from the 5DCH and 5DCH\* calculations is interesting. For low spin states such as  $0_1^+$  and  $4_1^+$ , the 5DCH and 5DCH\* calculations present a similar probability distributions. For higher states such as  $8_1^+$  and  $12_1^+$ , due to the reduction of the kinetic energy driven effect mentioned above, the 5DCH\* calculations present smaller average deformation  $\langle\beta\rangle$  and more concentrated probability distributions than those of 5DCH.

#### IV. SUMMARY

In summary, the five-dimensional collective Hamiltonian based on the covariant density functional theory has been first applied to investigate the phenomenon of the tidal wave in the yrast band of  $^{102}\text{Pd}$ . Although the 5DCH calculation with spin-independent MOIs could qualitatively describe the tendency of the yrast band, it

overestimates the increase of excitation energies (in turn underestimates the increase of MOIs) and the ratios of  $B(E2)/\mathcal{J}(I)$ . Considering that the adiabatic approximation adopted for the collective momenta up to the second order in the 5DCH may be not enough for the soft nucleus when the spin is large, the fourth order of the collective momenta in the collective Hamiltonian is taken into account. As a first attempt, a spin-dependent moment of inertia with the form of the *ab*-formula has been introduced into the collective Hamiltonian, and such a calculation is referred as the 5DCH\*. The experimental energy spectra, the spin-rotational frequency relation, the moments of inertia, as well as the ratios of  $B(E2)/\mathcal{J}(I)$  of the yrast band in  $^{102}\text{Pd}$  are well reproduced by the 5DCH\* calculations. That is, the 5DCH\* could well describe the general characteristics of the tidal wave.

The shape evolution for the tidal wave in  $^{102}\text{Pd}$  is analysed in the framework of the 5DCH-CDFT by giving the average quadrupole deformation parameters and the probability distributions of collective wave functions. It is found that the average deformation  $\langle\beta\rangle$  calculated by the 5DCH and 5DCH\* both increase linearly with spin, while the increase obtained by 5DCH is more obvious than that by the 5DCH\*. As analysed, this comes from the competition between the rotational kinetic energy  $\hat{T}_{\text{rot}}$  and the collective potential  $V$  and provides a schematic picture of the tidal wave.

In the present paper, by replacing the spin-independent MOIs with spin dependent MOIs, we effectively take the fourth order of the collective momentum into account and well describe the tidal wave in  $^{102}\text{Pd}$  with the collective Hamiltonian. One may argue that the MOIs calculated with the Thouless-Valatin terms [73] should be adopted rather than the Inglis-Belyaev formula, as the dependence of MOIs on deformation may become considerably complicated especially for

nuclei with soft potential energy surfaces [51, 64, 74, 75]. Such studies are undoubtedly meaningful, which can answer whether the spin dependent MOIs in the collective Hamiltonian are still necessary or not in this case. It is also noted that the mass parameters are just given from the cranking formula without any adjusted parameters. Although further consideration of Thouless-Valatin corrections might somewhat change the excited energies [73, 77], its influence on the behavior of the yrast band would be rather small. Anyway, this paper has presented a possibility that the higher order effect of collective momenta should be taken into account in the collective Hamiltonian.

### Acknowledgments

The authors are indebted to Jie Meng for constructive guidance and valuable suggestions. Fruitful discus-

sions with Fangqi Chen, Umesh Garg, Tamara Nikšić, Peter Ring, Dario Vretenar, Shipeng Xie, Zhenhua Zhang, and Pengwei Zhao are highly acknowledged. This work is partly supported by the Natural Science Foundation of China under Grants No. 11335002, No. 11375015, No. 11461141002, No. 11175002, No. 11235002, and No. 11005004, the Chinese Major State 973 Program No. 2013CB834400, and the China Postdoctoral Science Foundation under Grant No. 2015M580007.

- 
- [1] S. Frauendorf, J. Meng, and J. Reif, in *Proceedings of the Conference on Physics From Large  $\gamma$ -Ray Detector Arrays*, edited by M. A. Deleplanque (University of California Press, Berkeley, 1994).
  - [2] R. M. Clark and A. O. Macchiavelli, *Annu. Rev. Nucl. Part. Sci.* **50**, 1 (2000).
  - [3] S. Frauendorf, *Rev. Mod. Phys.* **73**, 463 (2001).
  - [4] H. Hübel, *Prog. Part. Nucl. Phys.* **54**, 1 (2005).
  - [5] J. Meng, J. Peng, S. Q. Zhang, and P. W. Zhao, *Front. Phys.* **8**, 55 (2013).
  - [6] S. Frauendorf, in *Proceedings of the Workshop on Gammasphere Physics; Berkeley, CA, 1-2 December, 1995*, edited by M. A. Deleplanque, I. Y. Lee, and A. O. Macchiavelli (World Scientific, Singapore, 1996, p.272).
  - [7] A. Bohr and B. R. Mottelson, *Nuclear structure* (Benjamin, New York, 1975, vol. II).
  - [8] S. W. Ødegård, G. B. Hagemann, D. R. Jensen, M. Bergström, B. Herskind, G. Sletten, S. Törmänen, J. N. Wilson, P. O. Tjøm, I. Hamamoto, et al., *Phys. Rev. Lett.* **86**, 5866 (2001).
  - [9] S. Frauendorf and J. Meng, *Nucl. Phys. A* **617**, 131 (1997).
  - [10] K. Starosta, T. Koike, C. J. Chiara, D. B. Fossan, D. R. LaFosse, A. A. Hecht, C. W. Beausang, M. A. Caprio, J. R. Cooper, R. Krücken, et al., *Phys. Rev. Lett.* **86**, 971 (2001).
  - [11] J. Meng and S. Q. Zhang, *J. Phys. G: Nucl. Part. Phys.* **37**, 064025 (2010).
  - [12] L. K. Pattison, D. M. Cullen, J. F. Smith, A. M. Fletcher, P. M. Walker, H. M. El-Masri, Z. Podolyák, R. J. Wood, C. Scholey, C. Wheldon, et al., *Phys. Rev. Lett.* **91**, 182501 (2003).
  - [13] D. M. Cullen, R. Glover, L. K. Pattison, P. M. Walker, S. Frauendorf, and D. Almeded, *J. Phys. G: Nucl. Part. Phys.* **31**, S1709 (2005).
  - [14] S. Frauendorf, Y. Gu, and J. Sun, *Int. J. Mod. Phys. E* **20**, 465 (2011).
  - [15] A. D. Ayangeakaa, U. Garg, M. A. Caprio, M. P. Carpenter, S. S. Ghugre, R. V.F.Janssens, F. G. Kondev, J. T. Matta, S. Mukhopadhyay, D. Patel, et al., *Phys. Rev. Lett.* **110**, 102501 (2013).
  - [16] S. Frauendorf, *Int. J. Mod. Phys. E* **24**, 1541001 (2015).
  - [17] S. Frauendorf, Cross-over between different symmetries, in *Fission and Properties of Neutron-Rich Nuclei*, , Proceedings of the Fifth International Conference on ICFN5, Sanibel Island, Florida, USA, 4-10 November 2012 (World Scientific, Singapore, 2014, p.39).
  - [18] W. Reviol, C. J. Chiara, M. Montero, D. G. Sarantites, O. L. Pechenaya, M. P. Carpenter, R. V. Janssens, T. L. Khoo, T. Lauritsen, C. J. Lister, et al., *Phys. Rev. C* **74**, 044305 (2006).
  - [19] W. Reviol, D. G. Sarantites, C. J. Chiara, M. Montero, R. V. Janssens, M. P. Carpenter, T. L. Khoo, T. Lauritsen, C. J. Lister, D. Seweryniak, et al., *Phys. Rev. C* **80**, 011304 (2009).
  - [20] A. O. Macchiavelli, A. D. Ayangeakaa, S. Frauendorf, U. Garg, and M. A. Caprio, *Phys. Rev. C* **90**, 047304 (2014).
  - [21] P. Ring, *Prog. Part. Nucl. Phys.* **37**, 193 (1996).
  - [22] D. Vretenar, A. V. Afanasjev, G. A. Lalazissis, and P. Ring, *Phys. Rep.* **409**, 101 (2005).
  - [23] J. Meng, H. Toki, S.-G. Zhou, S. Q. Zhang, W. H. Long, and L. S. Geng, *Prog. Part. Nucl. Phys.* **57**, 470 (2006).
  - [24] J. Meng, J. Y. Guo, J. Li, Z. P. Li, H. Z. Liang, W. H. Long, Y. F. Niu, Z. M. Niu, J. M. Yao, Y. Zhang, et al., *Prog. Phys.* **31**, 199 (2011) (in Chinese).
  - [25] H. Z. Liang, J. Meng, and S.-G. Zhou, *Phys. Rep.* **570**, 1 (2015).
  - [26] J. Meng and S.-G. Zhou, *J. Phys. G: Nucl. Part. Phys.* **42**, 093101 (2015).
  - [27] T. Nikšić, Z. P. Li, D. Vretenar, L. Próchniak, J. Meng, and P. Ring, *Phys. Rev. C* **79**, 034303 (2009).
  - [28] T. Nikšić, D. Vretenar, and P. Ring, *Prog. Part. Nucl. Phys.* **66**, 519 (2011).
  - [29] Z. P. Li, T. Nikšić, D. Vretenar, J. Meng, G. A. Lalazissis, and P. Ring, *Phys. Rev. C* **79**, 054301 (2009).

- [30] Z. P. Li, T. Nikšić, D. Vretenar, and J. Meng, Phys. Rev. C **80**, 061301 (2009).
- [31] Z. P. Li, T. Nikšić, D. Vretenar, and J. Meng, Phys. Rev. C **81**, 034316 (2010).
- [32] C. Y. Song, Z. P. Li, D. Vretenar, and J. Meng, Sci. China Phys. Mech. Astron. **54**, 222 (2011).
- [33] Z. P. Li, B. Y. Song, J. M. Yao, D. Vretenar, and J. Meng, Phys. Lett. B **726**, 866 (2013).
- [34] Z. P. Li, J. M. Yao, D. Vretenar, T. Nikšić, H. Chen, and J. Meng, Phys. Rev. C **84**, 054304 (2011).
- [35] J. Xiang, Z. P. Li, Z. X. Li, J. M. Yao, and J. Meng, Nucl. Phys. A **873**, 1 (2012).
- [36] J. J. Sun, Z. Shi, X. Q. Li, H. Hua, C. Xu, Q. B. Chen, S. Q. Zhang, C. Y. Song, J. Meng, X. G. Wu, et al., Phys. Lett. B **734**, 308 (2014).
- [37] T. Nikšić, P. Marević, and D. Vretenar, Phys. Rev. C **89**, 044325 (2014).
- [38] Z. H. Wang, J. Xiang, W. H. Long, and Z. P. Li, J. Phys. G: Nucl. Part. Phys. **42**, 045108 (2015).
- [39] Z. P. Li, T. Nikšić, D. Vretenar, P. Ring, and J. Meng, Phys. Rev. C **81**, 064321 (2010).
- [40] Z. P. Li, C. Y. Li, J. Xiang, J. M. Yao, and J. Meng, Phys. Lett. B **717**, 470 (2012).
- [41] Y. Fu, H. Mei, J. Xiang, Z. P. Li, J. M. Yao, and J. Meng, Phys. Rev. C **87**, 054305 (2013).
- [42] H. Mei, J. Xiang, J. M. Yao, Z. P. Li, and J. Meng, Phys. Rev. C **85**, 034321 (2012).
- [43] Z. Shi and S. Q. Zhang, Acta. Phys. Pol. B Proc. Suppl. **8**, 725 (2015).
- [44] B. A. Nikolaus, T. Hoch, and D. G. Madland, Phys. Rev. C **46**, 1757 (1992).
- [45] T. Bürvenich, D. G. Madland, J. A. Maruhn, and P. G. Reinhard, Phys. Rev. C **65**, 044308 (2002).
- [46] P. W. Zhao, Z. P. Li, J. M. Yao, J. Meng, Phys. Rev. C **82**, 054319 (2010).
- [47] P. Ring and P. Schuck, *The nuclear many-body problem* (Springer-Verlag, Berlin, 1980).
- [48] D. Inglis, Phys. Rev. **103**, 1786 (1956).
- [49] S. Beliaev, Nucl. Phys. **24**, 322 (1961).
- [50] M. Girod and B. Grammaticos, Nucl. Phys. A **330**, 40 (1979).
- [51] L. Próchniak and S. G. Rohoziński, J. Phys. G: Nucl. Part. Phys. **36**, 123101 (2009).
- [52] Q. B. Chen, S. Q. Zhang, P. W. Zhao, R. V. Jolos, and J. Meng, Phys. Rev. C **87**, 024314 (2013).
- [53] Q. B. Chen, S. Q. Zhang, P. W. Zhao, and J. Meng, Phys. Rev. C **90**, 044306 (2014).
- [54] Q. B. Chen, Acta. Phys. Pol. B Proc. Suppl. **8**, 545 (2015).
- [55] S. T. Belyaev, Nucl. Phys. **64**, 17 (1965).
- [56] M. Baranger and K. Kumar, Nucl. Phys. A **122**, 241 (1968).
- [57] M. Baranger and M. Veneroni, Ann. Phys. (N.Y.) **114**, 123 (1978).
- [58] D. L. Hill and J. A. Wheeler, Phys. Rev. **89**, 1102 (1953).
- [59] T. Une, A. Ikeda, and N. Onishi, Prog. Theor. Phys. **55**, 498 (1976).
- [60] A. Gózdź, K. Pomorski, M. Brack, and E. Werner, Nucl. Phys. A **442**, 26 (1985).
- [61] M. Matsuo, T. Nakatsukasa, and K. Matsuyanagi, Prog. Theor. Phys. **103**, 959 (2000).
- [62] N. Hinohara, T. Nakatsukasa, M. Matsuo, and K. Matsuyanagi, Prog. Theor. Phys. **119**, 59 (2008).
- [63] N. Hinohara, T. Nakatsukasa, M. Matsuo, and K. Matsuyanagi, Phys. Rev. C **80**, 014305 (2009).
- [64] N. Hinohara, K. Sato, T. Nakatsukasa, M. Matsuo, and K. Matsuyanagi, Phys. Rev. C **82**, 064313 (2010).
- [65] K. Matsuyanagi, M. Matsuo, T. Nakatsukasa, N. Hinohara, and K. Sato, J. Phys. G: Nucl. Part. Phys. **37**, 064018 (2010).
- [66] T. Marumori, Prog. Theor. Phys. **57**, 112 (1977).
- [67] T. Marumori, T. Maskawa, F. Sakata, and A. Kuriyama, Prog. Theor. Phys. **64**, 1294 (1980).
- [68] W. Pauli, *Handbuch der Physik*, (Springer-Verlag, Berlin, 1933, Vol. XXIV, p. 120).
- [69] L. Próchniak, K. Zajac, K. Pomorski, S. Rohoziński, and J. Srebrny, Nucl. Phys. A **648**, 181 (1999).
- [70] K. Kumar and M. Baranger, Nucl. Phys. A **92**, 608 (1967).
- [71] C. S. Wu and J. Y. Zeng, High Energy Phys. and Nucl. Phys. **9**, 214, (1985) (in Chinese).
- [72] C. S. Wu and J. Y. Zeng, Commun. Theor. Phys. **8**, 51 (1987).
- [73] J. Libert, M. Girod, and J.-P. Delaroche, Phys. Rev. C **60**, 054301 (1999).
- [74] L. Próchniak, P. Quentin, D. Samsen, and J. Libert, Nucl. Phys. A **730**, 59 (2004).
- [75] N. Hinohara, Z. P. Li, T. Nakatsukasa, T. Nikšić, and D. Vretenar, Phys. Rev. C **85**, 024323 (2012).
- [76] S. Frauendorf and J. Meng, Z. Phys. A **356**, 263 (1996).
- [77] E. K. Yuldashbaeva, J. Libert, P. Quentin, and M. Girod, Phys. Lett. B **461**, 1 (1999).